Membrane Stretch Affects Gating Modes of a Skeletal Muscle Sodium Channel

Iustin V. Tabarean, Peter Juranka, and Catherine E. Morris
Departments of Medicine and Biology, University of Ottawa, and Department of Neurosciences, Loeb Health Research Institute, Ottawa Hospital, Ottawa, Ontario K1Y 4E9, Canada

ABSTRACT The α subunit of the human skeletal muscle Na^+ channel recorded from cell-attached patches yielded, as expected for *Xenopus* oocytes, two current components that were stable for tens of minutes during 0.2 Hz stimulation. Within seconds of applying sustained stretch, however, the slower component began decreasing and, depending on stretch intensity, disappeared in 1–3 min. Simultaneously, the faster current increased. The resulting fast current kinetics and voltage sensitivity were indistinguishable from the fast components 1) left after 10 Hz depolarizations, and 2) that dominated when α subunit was co-expressed with human β1 subunit. Although high frequency depolarization-induced loss of slow current was reversible, the stretch-induced slow-to-fast conversion was irreversible. The conclusion that stretch converted a single population of α subunits from an abnormal slow to a bona fide fast gating mode was confirmed by using gigaohm seals formed without suction, in which fast gating was originally absent. For brain Na^+ channels, co-expressing G proteins with the channel α subunit yields slow gating. Because both stretch and β1 subunits induced the fast gating mode, perhaps they do so by minimizing α subunit interactions with G proteins or with other regulatory molecules available in oocyte membrane. Because of the possible involvement of oocyte molecules, it remains to be determined whether the Na^+ channel α subunit was directly or secondarily susceptible to bilayer tension.

INTRODUCTION

Voltage-dependent Na^+ channels are responsible for initiation and conduction of action potentials in nerve and muscle. The Na^+ channels are heteromers containing a large glycosylated peptide of 230–270 kDa (the α subunit) and smaller subunits of 33–38 kDa (β1 in muscle and β1 and β2 in brain). The β1 subunit, which is expressed both in brain and muscle, associates noncovalently to the α subunit in a 1:1 stoichiometry (Hartshorne and Catterall, 1984; Roberts and Barchi, 1987). Expression of the α subunit alone in *Xenopus* oocytes is sufficient to form functional voltage-gated Na^+ channels (Zhou et al., 1991; Moorman et al., 1990; Chahine et al., 1994). Na^+ channel α subunits from skeletal muscle (Skm1, both the rat and human homologs) (Zhou et al., 1991; Chahine et al., 1994) or rat brain (isoforms I, II, and III) (Smith and Goldin, 1998; Auld et al., 1988; Moorman et al., 1990;) expressed in oocytes yield currents displaying two components distinguished primarily by their inactivation properties. An abnormally slow component, usually representing the majority of the current, has an inactivation time constant an order of magnitude larger than that of the fast ("normal") component. The slow gating mode also displays a slower recovery from inactivation.

Single channel studies on oocytes expressing rat SkM1 α subunits (Zhou et al., 1991) or rat brain (IIA and III) α subunits (Krafte et al., 1990; Moorman et al., 1990) prove the existence of two gating modes: a slow gating mode in which channels undergo repeated openings and closings during the depolarizing pulse, and a fast gating mode in which the channel has brief openings and few reopenings during the depolarization. The ensemble averages of each mode correspond (respectively) to the slow and fast components of the macroscopic currents. Normal fast inactivation is restored when the α subunits (rat brain I, II, and rSkm1) are co-expressed with the β1 subunit (Isom et al., 1992; Smith and Goldin, 1998; Bennett et al., 1993). The human β1 subunit exhibits 96% identity with the rat homolog (McClatchey et al., 1993) and both interact functionally with either the rat or human Skm1 α subunits (Bennett et al., 1993; Cannon et al., 1993).

Ion channels displaying various types of mechanosensitive gating are ubiquitous, however little is known about their molecular identity. Recently it has been shown that various channels of known molecular identity display mechanosensitivity: the cardiac muscarinic K^+ channel (Ji et al., 1998), the S-type K^+ channel (Patel et al., 1998), the NMDA receptor (Casado and Ascher, 1998), and the *Shaker* K^+ channel (Gu et al., 1998). In this study we report on the effect of membrane stretch on human Skm1 Na^+ channels expressed in *Xenopus* oocytes.

Received for publication 4 March 1999 and in final form 11 May 1999.

Address reprint requests to Dr. Catherine E. Morris, Loeb Health Research Institute, Ottawa Hospital, 725 Parkdale Ave., Ottawa, Ontario K1Y 4E9, Canada. Tel.: 613-798-5555, ext. 8608; Fax: 613-761-5330; E-mail: cmorris@lri.ca.

© 1999 by the Biophysical Society

0006-3495/99/08/758/17 $2.00

MATERIALS AND METHODS

Channel expression in oocytes

The human Na^+ channel (hSkM1) was provided in the pSelect vector by R. Kallen with two mutations introduced at the C terminus to form two unique restriction sites. The original C terminal sequence, VRPGVKESLV, was mutated to VRPRVKEDLV. The hSkM1 was subsequently subcloned into the pSP64TM vector (I. MacLachlan, personal communication), a modified

version of pSP64T (Krieg and Melton, 1984) by digestion of hSkM1-pSelect with EcoRI, fill-in with Klenow polymerase, and ligation of the gel purified DNA into the EcoRV site of pSP64TM. The human Na^+ channel β1 subunit was provided by A. George in the pSP64T plasmid. The hSkM1-pSP64TM and the hβ1-pSP64T plasmids were linearized with EcoRI, and cRNA was synthesized from the SP6 promoter using a kit by Ambion. Oocytes were defolliculated by treatment with collagenase (Sigma Type IA, 2 mg/ml in calcium-free OR2 medium). Defolliculated stage V and VI oocytes were selected and injected with the hSkm1 cRNA (5–25 ng per oocyte). In some experiments, a 2:1 mixture of hSkm1 cRNA and hβ1 cRNA was injected. The oocytes were maintained at 18°C in OR2 solution supplemented with 100 μg/ml streptomycin and 100 IU/ml penicillin. The OR2 solution contained (in mM): 82.5 NaCl, 2.5 KCl, 1 $NaHPO_4$, 1 $CaCl_2$, 1 $MgCl_2$, 5 4-(2-hydroxyethyl)-1-piperazineethanesulfonic acid (HEPES-acid), pH 7.4. Oocytes were used for experiments after 1–5 days.

Electrophysiological recording

For patch clamp recording, the vitelline membrane was removed manually in a hyperosmolar solution (Methfessel et al., 1986) then the oocytes were returned to normal saline. We note that these patch clamp preparations necessitate three mechanical procedures (shrinkage, devitellination, reswelling) not performed on oocytes before two-microelectrode voltage clamp. Sodium currents were recorded using the cell-attached and inside-out configurations of the patch clamp technique (Hamill et al., 1981). Patch pipettes (1.5–2.5 MΩ) were made of borosilicate glass capillary tubes (Garner, Claremont, CA, 1.15 mm inner diameter) using a two-step vertical puller (model L/M-3P-A, List Medical, Darmstadt, Germany) and were coated close to the tip with a mixture of Parafilm (American Can, Greenwich, CT) and light and heavy mineral oil to reduce capacitance. The currents were recorded using an Axopatch 200B (Axon Instruments, Foster City, CA) patch clamp amplifier. Currents filtered at 5 kHz were digitized using an A/D converter (TL-1, Axon Instruments) and stored on the hard disk of a computer. Voltage pulse protocols were generated using a D/A converter (TL-1, Axon Instruments). The data acquisition software was pClamp6 (Axon Instruments). Current signals were corrected for linear capacitive currents with the compensation circuits of the amplifier and the residual capacitive and leakage currents were corrected by linear subtraction. In cell-attached and inside-out patches inward currents appear as positive deflections and outward currents downward deflections (opposite to the sign convention). The current traces were plotted as the original recordings (positive deflections represent inward currents) while the data presented in the *I-V* curves were corrected according to the sign convention.

The patch pipette solution contained (in mM): 140 NaCl, 1 KCl, 1 $MgCl_2$, and 5 HEPES, pH 7.4 with CsOH. Ca^{2+} was not included in the solution because it caused instability of the baseline (possibly Ca^{2+} permeating through endogenous channels activates Ca^{2+}-dependent Cl^- currents). The bath solution contained (in mM): 100 potassium aspartate, 20 KCl, 1 $MgCl_2$, 1 ethylene glycol-bis(β-aminoethyl ether) *N,N,N′,N′*-tetraacetic acid (EGTA), 5 HEPES-acid. The pH was adjusted to 7.4 with KOH. In some experiments a normal external solution containing (in mM): 140 NaCl, 5 KCl, 1.8 $CaCl_2$, 1 $MgCl_2$, 5 HEPES-acid was used as the bath solution. The pH was adjusted to 7.4 with NaOH. All experiments were performed at room temperature (21–23°C). Results are presented as means ± standard deviation (S.D.) and *n* represents the number of cells. All the chemicals were purchased from Sigma (St. Louis, MO). Measurement of pressure was done with a pneumatic transducer tester (model DPM-1B, Bio-Tek, Winooski, VT).

Data analysis

To provide a quantitative description of the two components the decaying part of the current traces was fitted with a weighted sum of two exponential functions using the Clampfit program (Axon Instruments). The Clampfit program was also used for area calculations; some curve-fitting was done and the graphs were produced with Sigmaplot4.0 (Jandel Scientific, San Rafael, CA). The peak current-voltage relationships were fitted to the following transform of a Boltzmann function (Favre et al., 1995):

$$I_{Na} = G_{max}(V - V_{rev})/\{1 + \exp[(V - V_{0.5})/\nu]\} \quad (1)$$

where I_{Na} is the peak Na^+ current elicited by the voltage pulse, V is the test potential, V_{rev} is the reversal potential, G_{max} is the maximal conductance, $V_{0.5}$ is the voltage for half-maximal activation, and ν is equal to the slope factor (in millivolts). This function assumes a simple two-state Boltzmann fit to the voltage-activation process and an ohmic conductance for the open channel. The inactivation curves were also fitted by a Boltzmann function:

$$I/I_{max} = 1/[1 - \exp(V - V_{0.5})/k] \quad (2)$$

where k and $V_{0.5}$ represent the slope factor and the half-maximal voltage for inactivation.

In the presence of Gd^{3+} (100 μM) the *I-V* of the Na^+ channels was shifted in the depolarizing direction by ~15 mV and the amplitude of the currents was reduced by ~50% (probably reflecting channel blockage as well). The effect of membrane stretch on Na^+ channel gating described below was obtained in the presence of Gd^{3+} (100 μM) as well; however, larger pressures were required to obtain comparable effects.

Previous studies using a two-electrode voltage clamp of oocytes reported that the biphasic time course of inactivation was variable such that a fast component was sometimes absent (Zhou et al., 1991). It seemed possible that as a consequence of the limited speed of the oocyte voltage clamp, the fast component could be missed in part or completely. In our patch clamp recording experiments we have circumvented this problem (the membrane capacitance is much smaller and faster settling times can be obtained).

RESULTS

Overview

In the *Xenopus* oocyte expression system, heterologous skeletal muscle Na^+ channel currents show an unpredictable mix of slow and fast components. Our aim was not to characterize this variability, but to study the effects of membrane tension on Na^+ channel behavior. As it turned out, however, the two issues—the component variability and the mechanical history of the patch—were intimately related. Accordingly, the results are presented as follows: first we report on the procedures used to characterize the kinetics and voltage dependence of slow and fast components, regardless of what fraction of the total current each constituted. Next we show that gigaohm seal formation, which subjects patches to variable amounts of membrane tension, was a critical factor in the slow-fast mix obtained. Thereafter, the results examine this effect, but instead of just "accidental" stretch (i.e., whatever was experienced during seal formation), elevated membrane tension was used as an experimental procedure.

Characterization and separation of the fast and slow gating modes

The high levels of expression of hSkm1 (α subunit) cRNA allowed us to measure macroscopic Na^+ currents from patches formed on oocytes. The currents displayed a biphasic decay, the fast component representing a variable pro-

portion of the current in different patches (the fast component was sometimes completely absent). Fig. 1 *A* shows, for a cell-attached patch, a family of currents elicited by 18-ms depolarizing steps from the holding potential of −110 mV to test potentials from −70 to 70 mV (in 10-mV increments). The potential applied across cell-attached patches was not affected by the resting membrane potential of the oocyte, which was 0 mV (the oocyte was maintained in high K^+ bath solution). Depolarizing steps were applied at 0.2 Hz. At higher frequencies the slow component disappeared during consecutive application of the test pulses, suggesting a slow recovery from inactivation in this gating mode. A similar finding was reported for the rSkm1 (Zhou et al., 1991). At 0.2 Hz, repeating the protocol did not change the currents. Currents in Fig. 1 *B* were from the same patch as Fig. 1 *A*, but here the same voltage step protocol was applied at 10 Hz and was run repeatedly. Each trace in Fig. 1 *B* represents the average of the last 3 runs in the series of 40 runs. The difference in rates of recovery from inactivation gives the opportunity to separate the two components of the currents. Fig. 1 *C* shows the currents obtained by subtracting the fast component (Fig. 1 *B*) from the total current (Fig. 1 *A*). It should be noted that in such experiments, after terminating the application of depolarizing pulses at 10 Hz, the slow component completely recovered within 3–5 min. At 0.2 Hz both current components were stable during most experiments, which usually lasted 5–15 min ($n = 45$). However, in some experiments ($n = 10$) a spontaneous change in the amplitude or shape of the current occurred at variable times after starting the experiment (20 s–15 min); these experiment were discontinued. For comparison, Fig. 1 *D* shows Na^+ currents from a patch obtained on an oocyte injected with both hSkm1 and hβ1. Here the entire current was in a fast gating mode (the "$\alpha+\beta$" mode). In some such patches, there was a slow component as well, but it was always of small amplitude, <10% of the peak current.

With hSkm1 alone, the entire Na^+ current of some patches was in the slow gating mode (Fig. 2 *C*). Data from such patches and from patches in which the fast and slow components were separated as described in Fig. 1, *A–C* were pooled and are presented in Fig. 2 *A* (*filled circles*) as normalized peak currents versus the test potential. The *I-V* curves show that the fast component (*open circles*) activated at more negative potentials than the slow component and that its voltage dependence was very similar to that of fast currents recorded from oocytes co-injected with hSkm1 and hβ1 (*triangles*). The *I-V* relationships were fitted with a Boltzmann function (Eq. 1, see Methods) which yielded the half-maximal voltages for activation of −27 mV for the slow gating mode, −47 mV for the fast gating mode, and −48 mV for the $\alpha+\beta$ mode. Fig. 2 *B* presents several currents from a cell-attached hSkm1-only patch in which both a fast and a slow component were present to approximately the same extent. A small current is detectable at −60 mV, and at −50 mV there is a current which inactivated completely. A slow component appears only at more positive potentials. For comparison, Fig. 2 *C* presents data from a cell-attached patch in which the currents were exclusively in the slow gating mode. In this patch the first measurable current was at −40 mV.

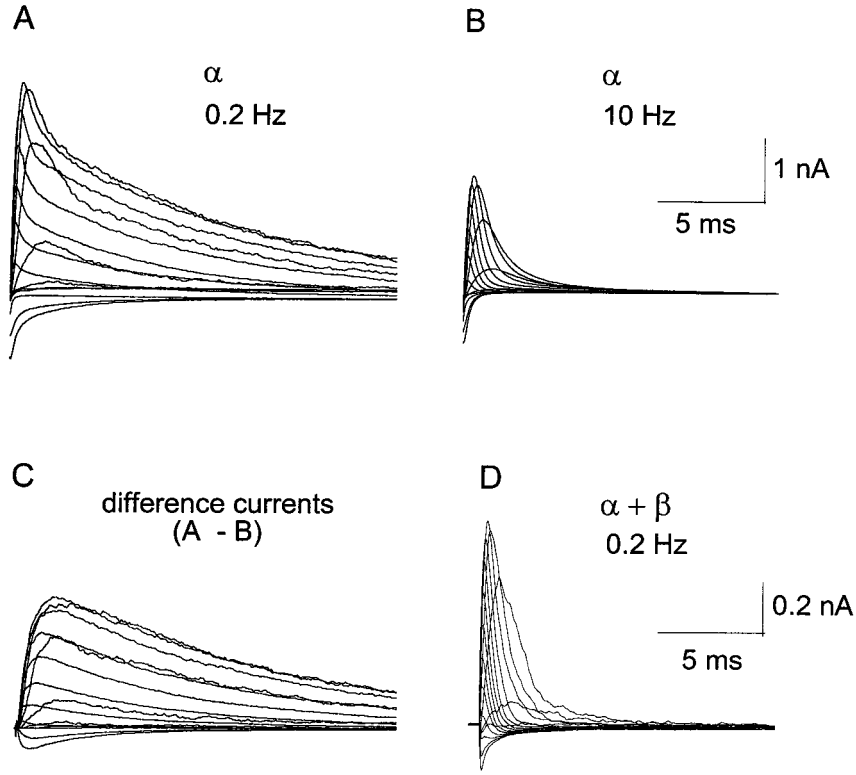

FIGURE 1 (*A*) A family of currents recorded in a cell-attached patch elicited by depolarizing steps from the holding potential of −110 mV to test potentials from −70 to 70 mV (in 10-mV increments). Inward currents appear as positive deflections and outward currents downward deflections (opposite to the sign convention). The depolarizing steps were applied at a frequency of 0.2 Hz. (*B*) Average currents of runs 38–40 from a series of 40 consecutive runs of the family of test pulses at 10 Hz. (*C*) Currents obtained by subtracting the fast component (*B*) from the total current (*A*). (*D*) shows typical Na^+ currents from a patch obtained on an oocyte injected with hSkm1 and hβ1 (frequency was 0.2 Hz).

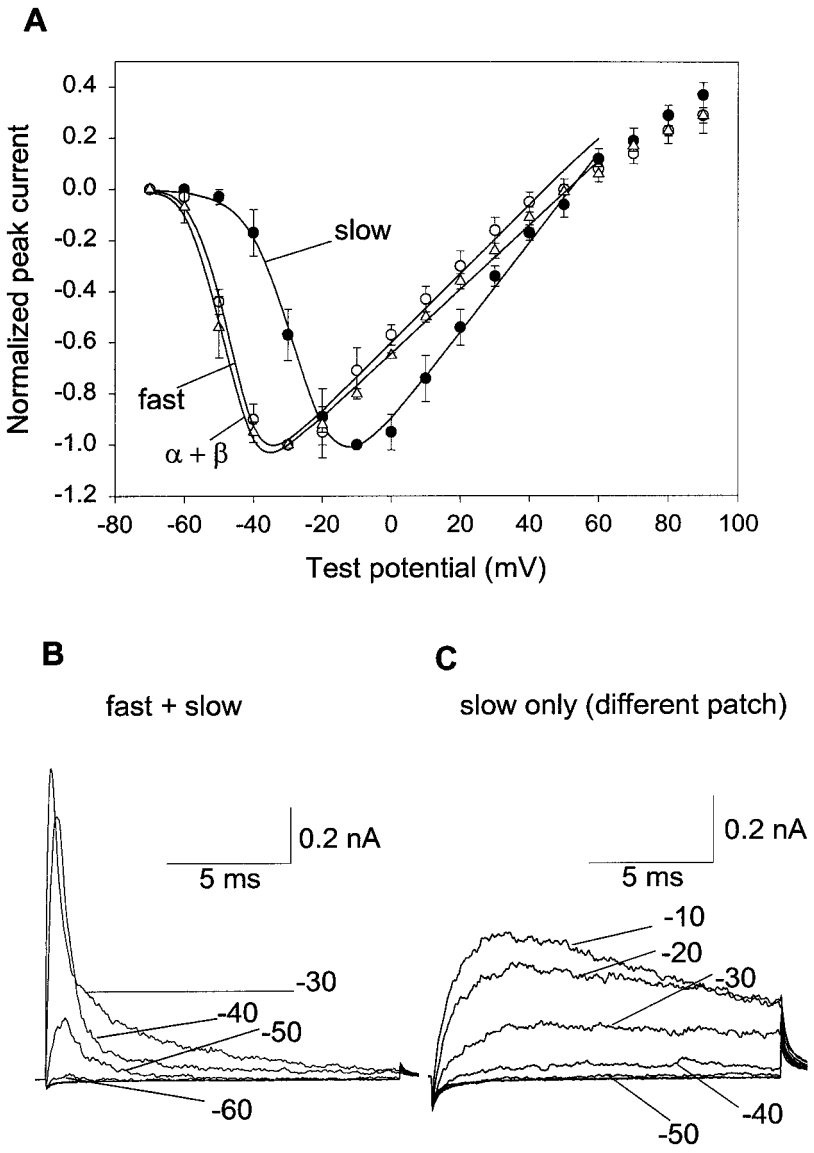

FIGURE 2 (*A*) *I-V* relationships for normalized peak currents: slow mode (*filled circles*, $n = 8$), fast mode (*open circles*, $n = 5$), and $\alpha+\beta$ mode (*open triangles*, $n = 4$); the continuous lines are Boltzmann fits (see Methods) which yielded $V_{0.5}$ for activation of -27 mV (slow), -47 mV (fast), and -48 mV ($\alpha+\beta$). (*B*) Currents elicited by depolarizing steps from the holding potential of -110 mV to the indicated test potentials. Both the fast and slow gating modes are present in this cell-attached patch. (*C*) Slow gating mode currents recorded in a cell-attached patch elicited by depolarizing steps from the holding potential of -110 mV to the indicated test potentials.

The ability to separate the two gating modes facilitated their further characterization (Figs. 3 and 4). The time to peak (Fig. 3 *A*) of the slow component was larger than that of either the fast component or of the $\alpha+\beta$ mode. τ of decay (Fig. 3 *B*), obtained by fitting a single exponential to the decay phase of the currents showed little voltage dependence for the slow component. Steady-state inactivation for the slow, fast, and $\alpha+\beta$ mode was examined using a double-step protocol: a 200-ms conditioning pre-pulse at potentials between -110 mV and -10 mV was followed by a 10-ms test pulse at 0 mV. The steps were applied at 0.2 Hz. With increasing depolarization of the pre-pulse, two discrete effects were noted (Fig. 4 *A*): the overall amplitude of the currents elicited by the test step decreased, and the fast component disappeared. At 0.2 Hz, the fast component disappeared "sooner," i.e., at more negative pre-pulse potentials than the slow component (Fig. 4 *A*). In order to separate the slow and fast components an approach similar to that used for the *I-V* curves was used: pulses were applied at 10 Hz, causing the slow component to disappear (Fig. 4 *B*). Subtracting these 10 Hz currents from the initial (0.2 Hz) currents (Fig. 4 *A*) leaves only slow test currents (Fig. 4 *C*). As before, these data were pooled with data from patches where only a slow component was present. In order to correct the peak currents of the fast component (as in Fig. 4 *B*) for the residual slow component, a scaled slow component, from the same patch, was subtracted. The steady-state inactivation curves were fitted with a Boltzmann function (Eq. 2, see Methods) which yielded the half-maximal voltages for inactivation: -55 mV for the slow gating mode, -74 mV for the fast gating mode, and -77 mV for the $\alpha+\beta$ mode.

The proportion of fast gating mode present in a patch is affected by the patch formation history

The formation of gigaseals on oocytes sometimes occurs spontaneously upon touching the membrane. Other times it

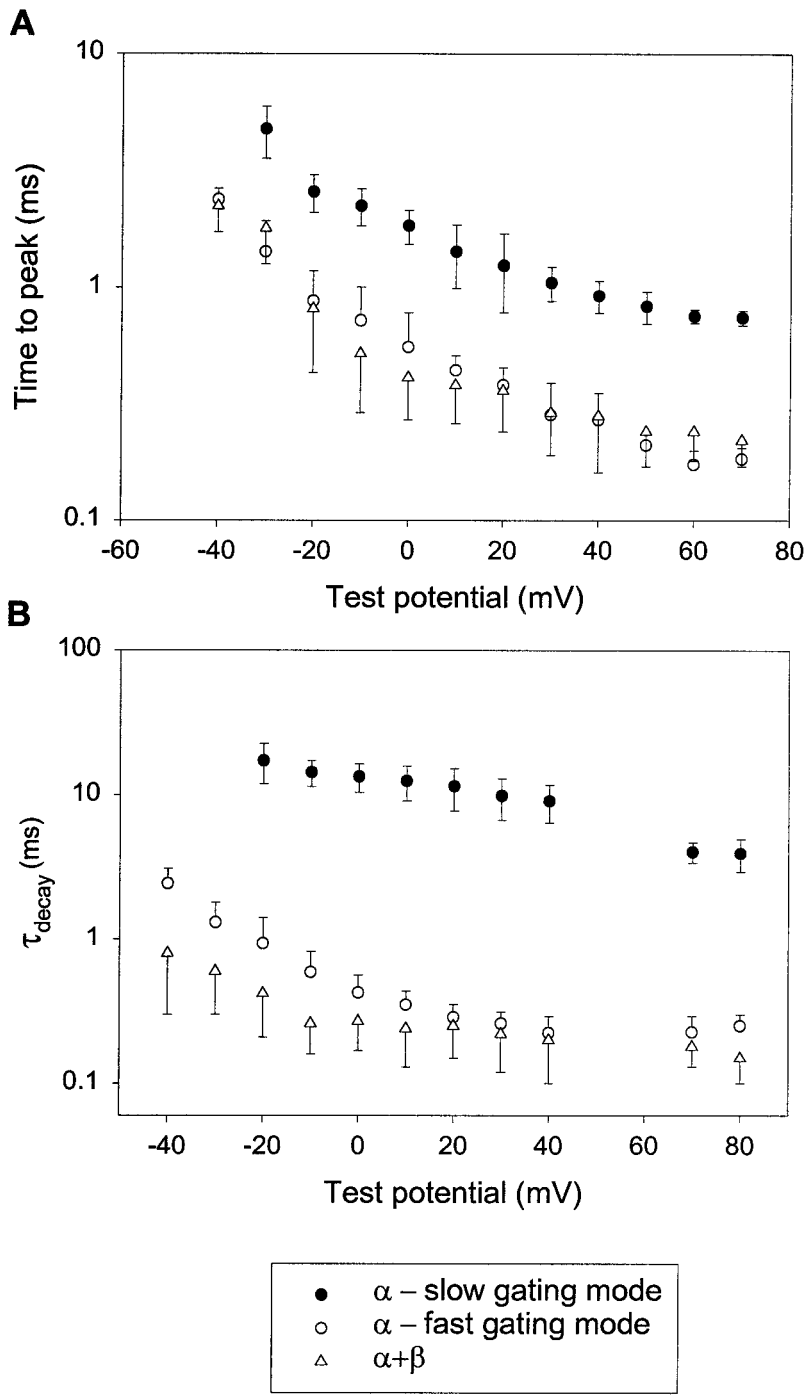

FIGURE 3 Voltage dependence of the time to peak (*A*), and τ of decay (*B*) for the slow gating mode (*filled circles*, $n = 6$), fast gating mode (*open circles*, $n = 5$), and $\alpha+\beta$ mode (*open triangles*, $n = 3$). Close to the reversal potential (~50 mV), currents were too small for fitting.

requires the application of suction through the patch pipette. We observed a correlation between the amount of suction applied and the proportion of the fast component recorded in the patch: if pressures > -10 to -15 mmHg were applied there was always a fast component. In patches obtained from the same oocytes without applying any negative pressure there was less or no fast component. Fig. 5 *A* illustrates this finding: the currents in a and b were recorded from patches in which patch formation was spontaneous, while the ones in c and d were recorded from patches that required pressure for seal formation (-15 mmHg and -25 mmHg, respectively). The currents in a–d were recorded using 0.2 Hz in four cell-attached patches from the same oocyte; similar results were observed in 10 of 10 oocytes in which the same experiment was performed.

We also noticed that in oocytes expressing large currents (the current in the patch ~1 nA or larger) the fast component was always present regardless of whether patches were

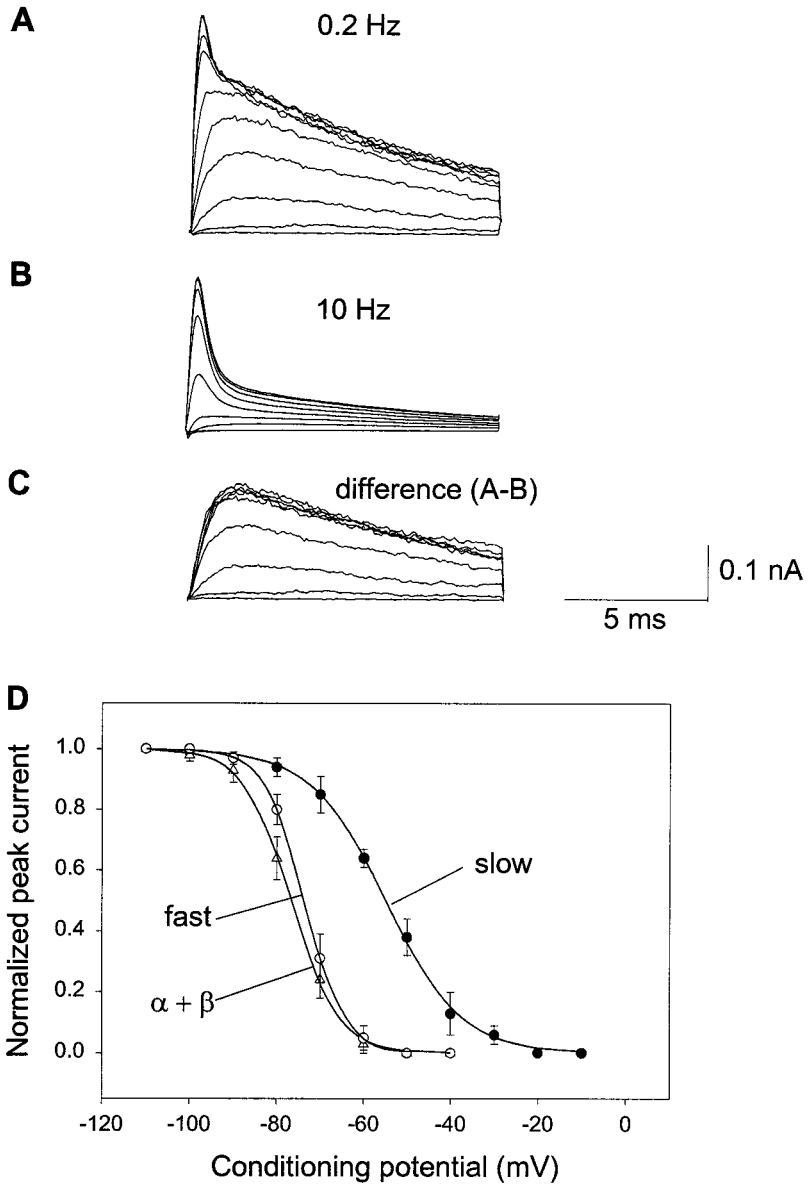

FIGURE 4 (*A* and *B*) Currents elicited by test pulses in a cell-attached patch from an oocyte injected with hSkm1 using steps applied at the indicated frequencies. A double-step protocol was used: a 200 ms conditioning pre-pulse to potentials between −110 mV, and −40 mV was followed by a test pulse to Na^+ 0 mV. (*C*) Subtracting the currents in (*B*) from those in (*A*) leaves only slow currents. (*D*) Normalized steady-state inactivation curves for the slow mode (*filled circles*, $n = 7$), fast mode (*open circles*, $n = 4$), and $\alpha+\beta$ mode (*open triangles*, $n = 3$). The continuous lines are Boltzmann fits which yielded $V_{0.5}$ for inactivation of −55 mV (slow), −74 mV (fast), and −77 mV ($\alpha+\beta$).

obtained without applying suction. Fig. 5 *B* shows families of currents from two patches obtained spontaneously from oocytes expressing large Na^+ currents.

Membrane stretch causes a shift toward the fast gating mode

To test whether membrane stretch was affecting the presence of the fast component, we applied suction to patches on which gigaseals were obtained spontaneously. Fig. 6, *A–C* shows Na^+ currents from three patches stimulated at 0.2 Hz before (*left*) and after (*right*) application of −30 mmHg for 1 or 2 min. The Na^+ currents switched completely from a slow gating mode to a fast gating mode and remained in a fast mode after the release of pressure. After such a stretch-induced switch, no recovery of the slow gating mode was observed even when observations continued up to 30 min. In six patches that were initially "slow only," sufficient suction was applied to obtain complete stretch-induced conversion from slow only to fast only. Of these, four showed a decrease (24 ± 12%) in peak current while two showed an increase (31 ± 16%). Suction also reduced the slow component in patches (e.g., Fig. 9 *A*) in which there was a mixed fast/slow component at the outset. In 11 such patches, sufficient stretch was applied to obtain a complete stretch-conversion to fast mode; of these, the peak current decreased (22 ± 10%) in seven and increased (14 ± 5%) in four patches. Stretch-induced switching to fast gating was also observed in an additional eight patches, which were lost before complete conversion was achieved. In all experiments the stability of the current was monitored for 3–4 min before application of suction (e.g., Fig. 10 *A*).

To compare this fast gating mode with that observed in control conditions we characterized its voltage dependence

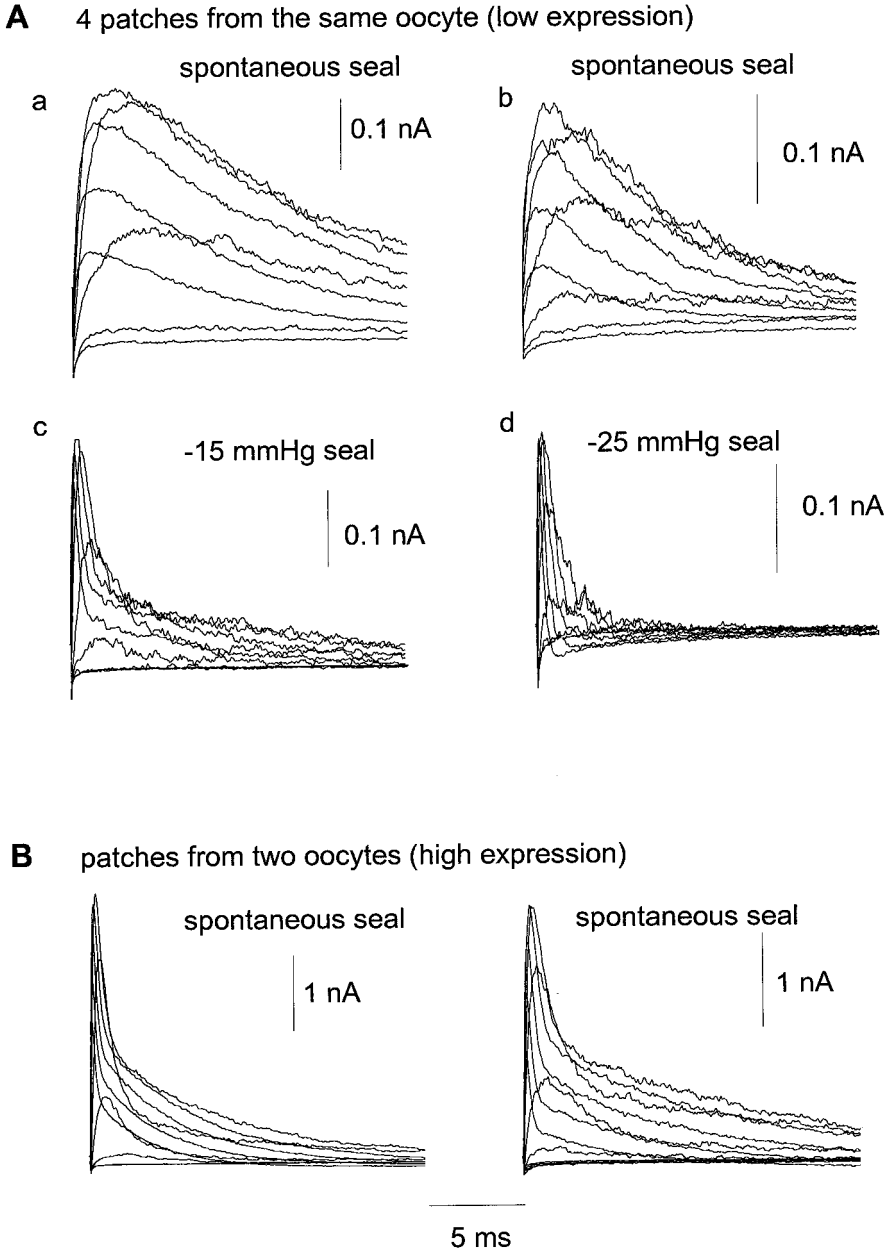

FIGURE 5 Families of Na^+ currents elicited by step depolarizations from a holding potential of −110 mV to test potentials ranging between −70 mV and 20 mV. (*A*) Currents recorded from four patches made on the same oocyte: patch formation required no suction (a, b, "spontaneous seal"), −15 mmHg (c) or −25 mmHg (d), as indicated. (*B*) Currents from two patches obtained spontaneously from two oocytes expressing large Na^+ currents.

and kinetics. Fig. 7, *A* and *B* compare the activation and the inactivation characteristics of the suction-induced fast gating mode (*open circles*) with the ones for the fast and slow gating modes described above (Figs. 2–4). The curves nearly coincide with the ones for the fast gating mode in control conditions, the half-maximal voltages for activation (Fig. 7 *A*) and inactivation (Fig. 7 *B*) being −49 mV and −78 mV, respectively. In Fig. 7 *C*, the τ of decay (single exponential fit to the decay phase of the currents) is compared over a range of voltages for control fast currents and those obtained by stretching the membrane; they are not statistically distinguishable. The two fast gating modes thus have identical kinetics, and their voltage dependence of activation and inactivation are the same. There is no reason to argue that they are not identical.

The time course of stretch-induced changes was also examined. First, Fig. 8, *A–C* compare fast currents from the same patch before and after suction. Initially (Fig. 8 *A*), both gating modes were present in the patch; the slow gating mode could be reversibly eliminated by applying a depolarizing step to 0 mV at 10 Hz. By the third step the slow component could no longer be detected, only a small fast component remained. After complete recovery of the current, −25 mmHg was applied inside the pipette and maintained. Meanwhile, the patch was depolarized to 0 mV at 0.2 Hz and a progressive decrease in the slow component was observed (Fig. 8 *B*). By the eighth depolarizing step (i.e., ~35 s after suction was applied) the slow component disappeared completely, leaving only a fast current. In Fig. 8 *C* this residual current is superimposed on the

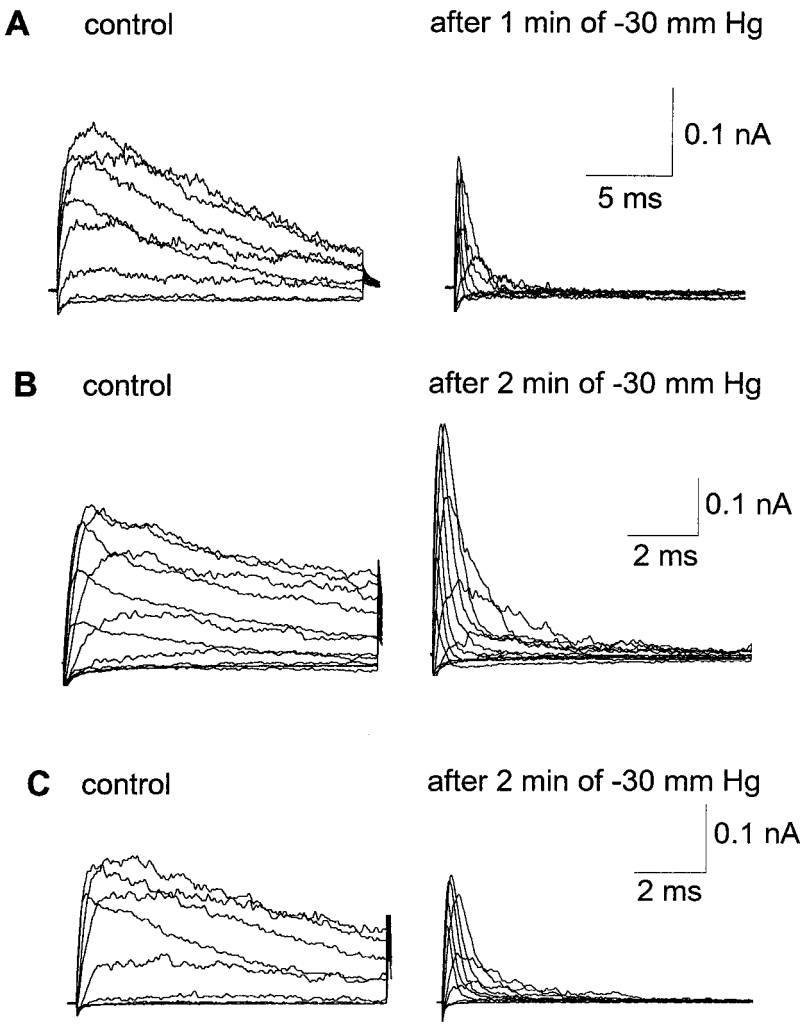

FIGURE 6 For three different patches obtained without suction (*A–C*), Na^+ currents recorded before (control), and after (right) application of −30 mmHg for the indicated times.

third fast current in Fig. 8 *A* along with a second version of it (*dotted line*), scaled up to the peak of the ninth with-suction current.

Figs. 9 and 10 *B* illustrate more fully how the suction-induced switch in gating mode developed gradually while pressure was maintained. The decaying phase of the currents elicited during a sustained −30 mmHg suction (Fig. 9 *A*) was fitted with a weighted sum of two exponentials (Fig. 9 *B*) and the fast and slow time constants are plotted as a function of time in Fig. 9 *C*. The τ fast remained constant (~0.3 ms), whereas τ slow decreased over time during suction (steps were applied at 0.2 Hz) but stabilized at an order of magnitude larger (~2 ms) than τ fast. Because τ slow decreased with time (this trend was present in all the patches studied, as will be seen in Fig. 11 *B*) it was inappropriate to use the relative weights of the two components of the double exponential fits to compare different traces. Instead, to quantify the gradual decrease of the slow component we used the total charge carried by it (the area enclosed by the slow component trace and the *x* axis) (Fig. 9 *C*, *filled diamonds*). After complete conversion to the fast gating mode (the 30th step) suction was released and no recovery was observed (Fig. 9 *C*). It is noticeable that once the slow component decreases to <10% (~the 20th step) its time constant (*open triangles*) displays some variability; this is because for small currents the fit is less reliable.

A similar experiment is presented in Fig. 10. Before application of suction the current was stable during depolarizing steps to 0 mV (Fig. 10 *A*), and started to decrease upon application of −20 mmHg. By the seventh step (i.e., ~35 s) after the application of suction the effect reached a plateau (Fig. 10 *B*). The pressure was released and, after 30 s, −30 mmHg was applied. The pressure effect developed completely: after ~30 s there was only a fast component left (Fig. 10 *C*). After the pressure was released no recovery of the slow gating mode was observed (Fig. 10 *D*). Fig. 10 *E* shows the decrease of the total charge carried by the slow component. The total charge decreased faster at −30 mmHg that at −20 mmHg. Some recovery can be observed after the first application of pressure (−20 mmHg). Partial recovery was also observed in three other patches, but, as in Fig. 9, only at low pressures (−10 to −20 mmHg), which did not cause a complete switch to the fast gating mode. For patches (n = 17) in which a complete conversion to fast mode was obtained, no recovery was observed.

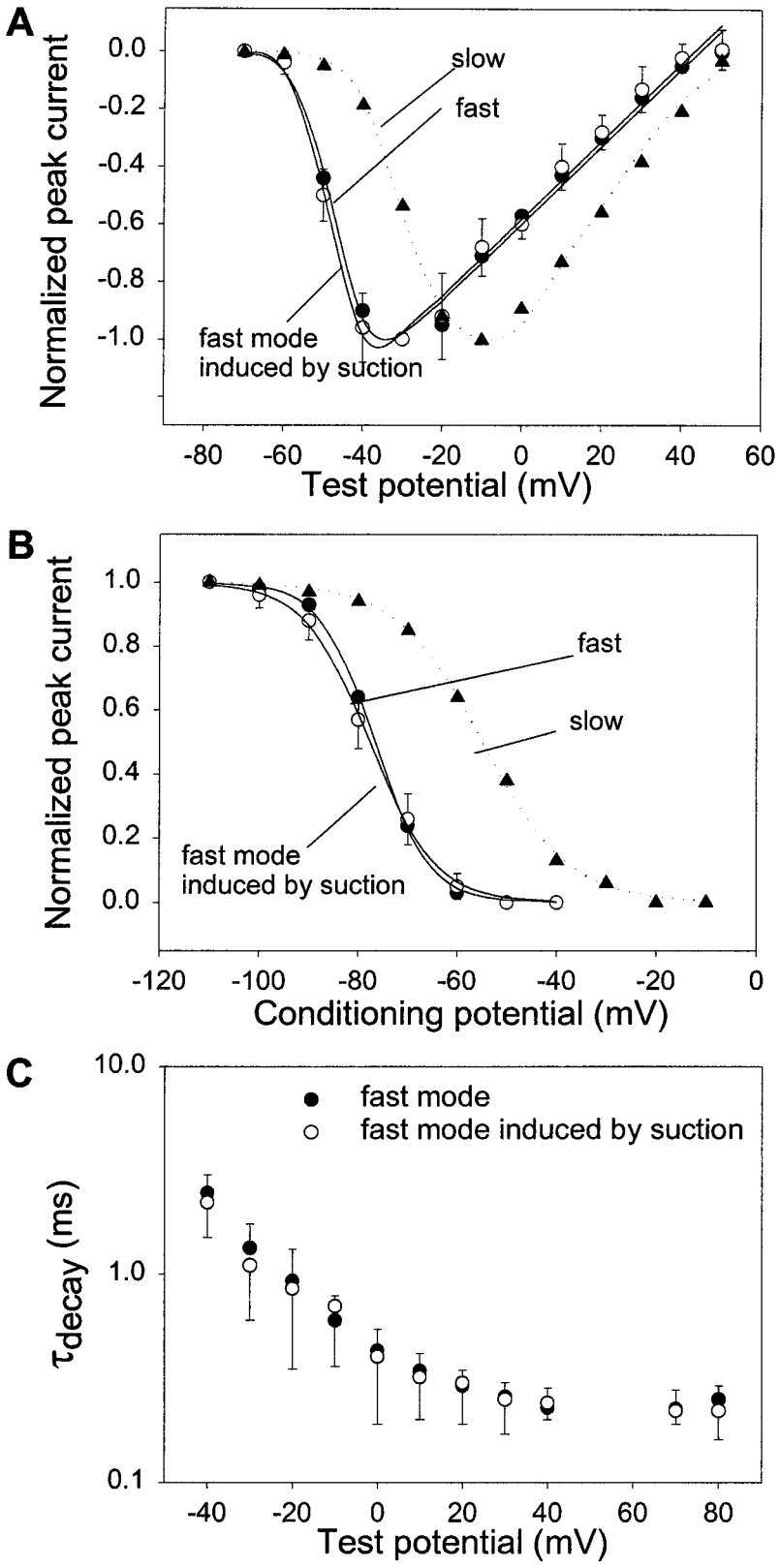

FIGURE 7 (*A*) *I-V* relationship for normalized peak currents of the fast gating mode obtained by applying suction (*open circles*, $n = 5$). The data were fitted to a Boltzmann function, yielding $V_{0.5}$ for activation of −49 mV. For comparison, *I-V* relationships for the fast and slow gating modes described above (Fig. 2) are replotted. (*B*) Normalized steady-state inactivation relations for the fast mode (*open circles*, $n = 5$). Fitting to a Boltzmann function yielded a $V_{0.5}$ for inactivation of −78 mV. Inactivation curves for the fast and slow gating modes described above (Fig. 4) are replotted. (*C*) shows the τ of decay for the fast gating mode induced by suction (*open circles*, $n = 5$) along with the replotted control fast mode (*filled circles*) from Fig. 3. Close to the reversal potential (~50 mV) the currents were too small for fitting.

The rate at which the effect of pressure decreased the amplitude of the slow component was dose-dependent (the larger the pressure, the faster the effect developed). Fig. 11 *A* shows the time course of decay of the total charge carried by the slow component from five different patches. Although the time course showed variability from patch to patch it is obvious that the rate was greater for the larger pressures. Also, it should be noted that the effect of pressure

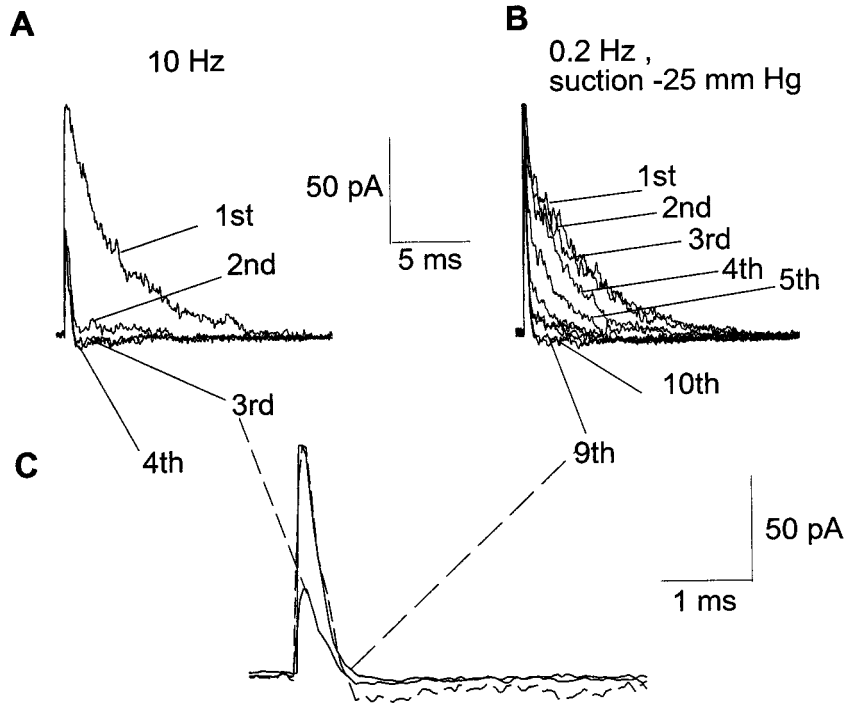

FIGURE 8 (*A*) Na^+ currents elicited by depolarizations to 0 mV delivered at 10 Hz. Initially ("1st") both gating modes were present in the patch, but the slow component disappeared after two pulses, leaving only a small fast component. (*B*) After full recovery of the slow component from inactivation, −25 mmHg suction was applied and maintained while the membrane was stepped to 0 mV at 0.2 Hz. The slow component decreased gradually, and by ~35 s after suction was applied (i.e., after the eighth step) disappeared completely, leaving only fast current. (*C*) compares the time course of the fast current obtained by using 10 Hz (to reversibly inactivate the slow component ("3rd")) prior to suction and the fast current obtained by suction ("9th"); the dashed line current is a scaled-up version of the 3rd from (*A*).

developed with a delay of at least 5 s after the application of pressure. This delay could not be quantified precisely because the patch could not be depolarized more frequently than every 5 s (0.2 Hz) (the slow gating mode recovers slowly from inactivation). Fig. 11 *B* displays the time dependence of the slow (*open symbols*) and fast (*filled symbols*) time constants obtained by a double exponential fit from the same patches. The initial τ_{decay} for the slow component varied from patch to patch and did not decrease smoothly during suction. There was, however, in every patch a trend to decrease during suction. Preliminary data on the rat brain IIA α subunit (the cDNA was a generous gift of Robert Dunn) expressed in oocytes indicated a similar effect of stretch, as was observed for the human SkM1 α subunit: a shift to fast gating modes (data not shown).

DISCUSSION

Overview

Expressed in *Xenopus* oocytes, the α subunit of the skeletal muscle Na^+ channel exhibits an unpredictable mix of fast and slow gating modes. Although slow mode gating is anomalous in skeletal muscle, some neuronal and glial Na^+ channels exhibit slow mode behavior in vivo (Taylor, 1993). Our main finding was that membrane stretch induced an irreversible conversion from the slow to the fast gating mode in the Na^+ channel α subunit. The stretch-induced fast mode was indistinguishable kinetically and its voltage dependence from the fast gating mode observed 1) in patches that had both fast and slow current but were left with fast current only after depolarizing steps at 10 Hz frequency had reversibly inactivated the slow component, and 2) in patches from oocytes co-expressing the β subunit with the α subunit.

When oocytes expressed low levels of current, patches whose gigaseals formed spontaneously (no suction) exhibited predominantly slow mode currents and some had purely slow currents. Several minutes of stretch irreversibly changed these slow-only currents to "fast-only." This we view as a conversion of a single population of channels from one gating mode to another. By forming multiple patches on the same oocyte, we established that if suction was used during gigaohm seal formation it was responsible for starting the process of stretch-conversion. Thus, in a typical patch, the fast-slow mix probably included a fast component that had been inadvertently stretch-induced. Likewise, the simplest interpretation of what ensued when stretch was subsequently applied as an experimental procedure is the following: stretch caused a resumption of the conversion that had commenced during seal formation only to be interrupted when suction was released following seal formation. This would be akin to the events illustrated in Fig. 10. The realization that stretch alters gating behavior of the sodium channel is important because it demonstrates that membrane tension can have impacts on integral membrane proteins whose functions are unrelated to mechanotransduction. Additionally, the fact that an agent (stretch) could rapidly convert pure-slow patch currents to pure-fast has implications about the gating repertoire of the α subunit.

Comparisons with other studies

Before speculating on how membrane stretch may have acted on the Na^+ channel, we need to place our results in

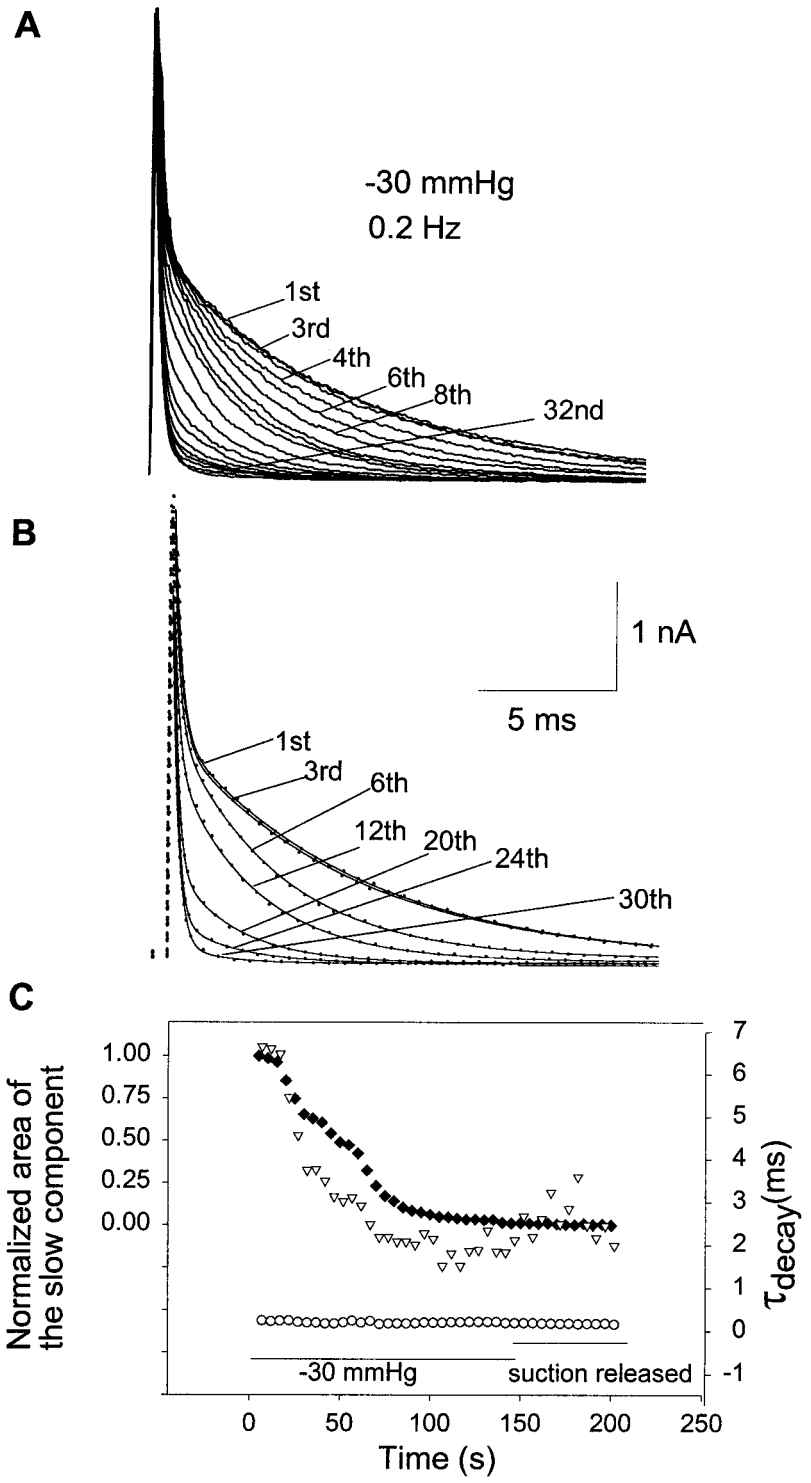

FIGURE 9 (*A*) Gradual suction-induced switch to the fast gating mode. Suction (−30 mmHg) was applied and maintained after the first depolarizing step. The patch was stepped at 0.2 Hz to 0 mV from a holding potential of −110 mV. (*B*) The decaying phase of the currents was fitted with a weighted sum of two exponentials (*dotted lines* represent current data, *solid lines* represent double-exponential fits). Time constants for the two exponentials illustrated are 0.25 and 6.65 ms (1st step); 0.24 and 6.47 ms (3rd); 0.21 and 4.57 ms (6th); 0.24 and 2.92 ms (12th); 0.20 and 2.15 ms (20th); 0.22 and 1.87 ms (24th); and 0.20 ms (30th step, no slow component was present). (*C*) The fast (*open circles*) and slow (*open triangles*) time constants are plotted as a function of time (5 s between steps). The normalized total charge (*filled diamonds*) carried by the slow component (area enclosed by the current trace, and the zero-current *x* axis) is also plotted as a function of time. After the 32nd step, suction was released.

the context of previous reports. Using either "accumulated inactivation" of slow mode channels or membrane stretch, we separated and characterized the two gating modes. The fast gating mode obtained by membrane stretch was distinguishable neither from the fast component observed without stretch nor from the $\alpha+\beta$ mode. The $V_{0.5}$ values for both activation and inactivation of the slow mode were ~20 mV more positive than for the fast mode. Distinct activation (Fleig et al., 1994) and inactivation (Krafte et al., 1988; Hebert et al., 1994; Fleig et al., 1994) $V_{0.5}$ values for slow and fast gating modes have been reported previously. For both gating modes, our $V_{0.5}$ values for activation and inactivation were ~10 mV more negative than reported in other studies, probably because we used Ca^{2+}-free pipette solution (see Methods). Our finding that activation kinetics differed for the two gating modes (the time to peak was

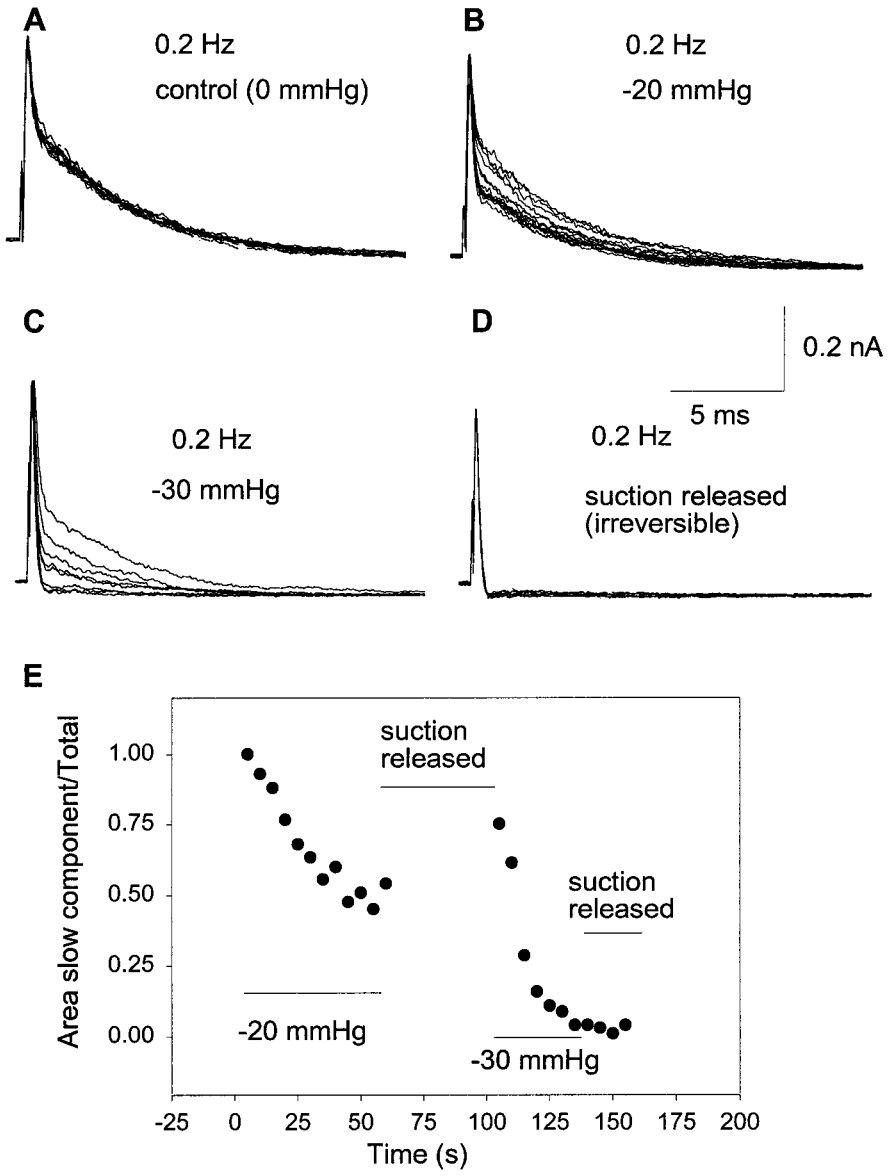

FIGURE 10 (*A*) Control for the stability of the current before suction during steps to 0 mV from −110 mV at 0.2 Hz. (*B*) Upon application of −20 mmHg the slow component decreased, and reached a steady-state by the seventh step (i.e., ~35 s). (*C*) Thirty seconds after suction at −20 mmHg suction was released, −30 mmHg was applied. After ~30 s at the higher suction, only a fast component remained. (*D*) After the pressure was released no recovery of the slow gating mode was observed. (*E*) The fraction of total charge carried by the slow component is also plotted as a function of time.

larger for the slow mode) is consistent with a single channel report by Zhou et al. (1991) for rat Skm1 showing that the slow mode has a longer latency to first opening.

When a mode conversion was in progress (e.g., Fig. 9), it was not just the relative weight of the slow component that changed, but its τ_{decay}. Nevertheless, even at its smallest this τ_{decay} exceeded by an order of magnitude that of the fast component. For simplicity we refer to the continuum of slow modes as "the" slow mode. If the nonconstant nature of τ_{decay} indicates the existence of additional gating modes and reflects states of the channel intermediate between slow and fast, this would be consistent with previous suggestions (Zhou et al., 1991) for more than two gating modes in rat Skm1. Like Zhou et al. (1991) we found that varying the proportion of constant fast and slow components cannot fit the current traces for all patches or for all conditions for one patch.

Consistent with observations for both rat brain Na^+ channels (Krafte et al., 1990) and rat Skm1 (Zhou et al., 1991), in our experiments with human Skm1, the level of expression in oocytes was correlated with the relative amount of fast component: the larger the current expressed, the larger the proportion represented by the fast component. However, at very large current expression levels, for human Skm1 (as for the two rat channels) a prominent slow component was always observed.

Peak current before and after suction-induced mode conversion

Fleig et al. (1994), who describe a gradual switch to fast gating in excised macropatches, reported that the conversion was associated with an increase in peak currents in only 4 of 10 patches. We too obtained similarly variable results for this parameter, with less than half of patches showing an increase in peak currents after complete conversion from slow to fast gating.

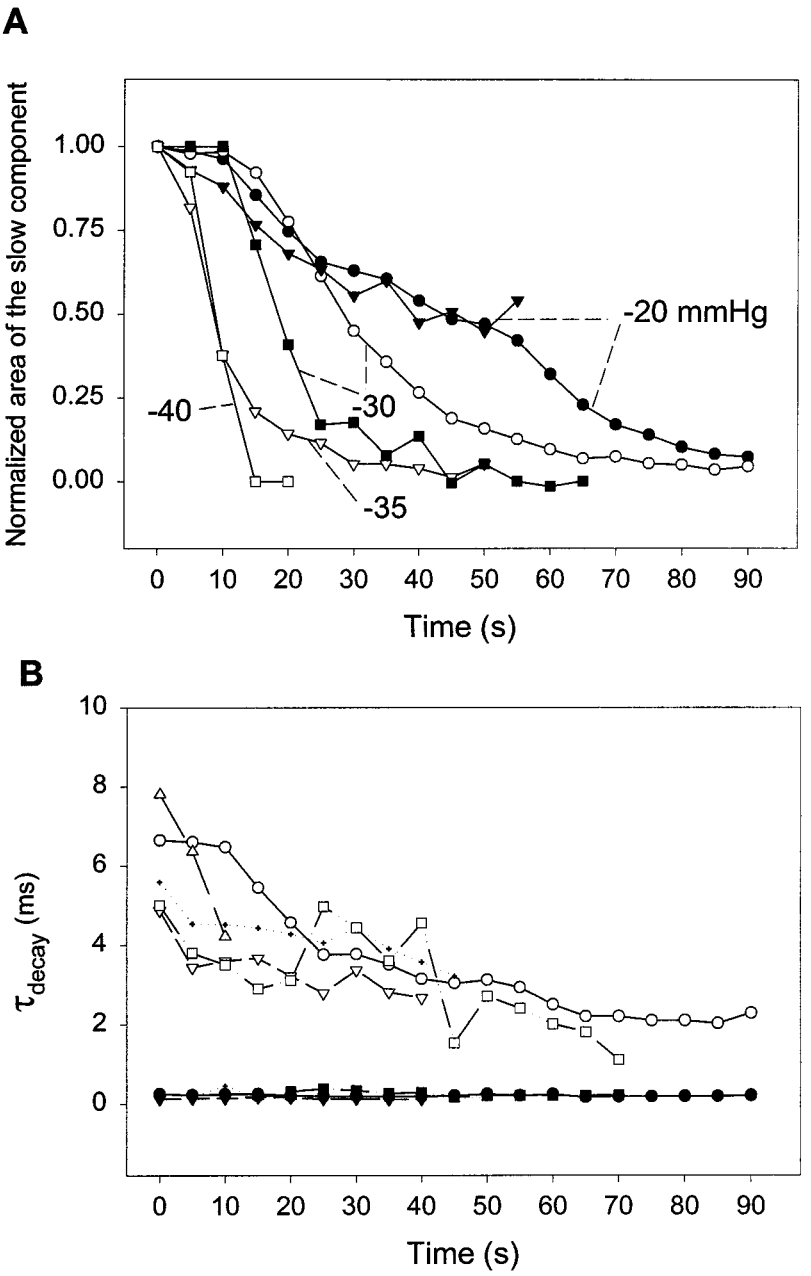

FIGURE 11 (*A*) Data (normalized) from five cell-attached patches for the total charge carried by the slow component are plotted as a function of time while various amounts of suction (as indicated in mmHg) were applied. (*B*) Time courses of the slow (*open symbols*), and fast (*filled symbols*) time constants obtained by a double exponential fit. Data are from the same patches as in (*A*)

Should peak values change? *I-V* relations showed that fast mode currents were maximal at more negative potentials than slow mode currents. Based on the larger driving force for Na^+ at the more negative voltages, post-conversion (fast) peak currents should thus be larger than the pre-conversion (slow) ones. For instance, assuming both gating modes reverse at +55 mV, and given that maximal currents are obtained at −30 mV and −10 mV for the fast and slow modes, respectively, the expected increase would be 85/65 = ~1.3-fold.

A possible explanation for the decrease in peak currents seen in more than half of patches is that not all the Na^+ channels present in the patch are open at the peak. A fraction may have already inactivated (Gonoi and Hille, 1987; Cota and Armstrong, 1989) such that the proportion of channels open at the peak may be larger for the slow mode. Additionally, a decrease in current could be caused by a loss of functional channels (rundown) during stretch. This is not to suggest, however, that a suction-induced rundown of slow gating channels could, on its own, explain our results, since we always obtained fast-only out of slow-only currents.

Possible mechanisms by which membrane tension alters Na^+ channel gating

Although the mechanism for the membrane-stretch induced conversion of the sodium channel α subunit to a faster gating mode cannot be resolved from these experiments,

several possibilities can be considered. In doing so, it is critical to keep in mind the essential irreversibility of the slow-to-fast conversion. Although a small degree of reversibility was noted for small mechanical stimuli, the conversion was predominantly unidirectional. Stretch-activation and stretch-inactivation of mechanosensitive (MS) channels, by contrast, are generally reversible (Sachs and Morris, 1998), as if elevated membrane tension provides gating energy. Even in MS channels, however, hysteresis, which could be viewed as partial irreversibility, is not uncommon. There is one well-documented irreversible effect of prolonged stretch on MS channels, namely the abolition of adaptation in the MS cation channels of oocytes (see Hamill and McBride, 1997). Thus, the finding of an irreversible stretch effect on ion channel gating modes is not without precedent, but this is the first report for a molecularly identified channel.

Several classes of irreversible mechanisms could be invoked to explain our data; the ones suggested here are not mutually exclusive. First, membrane stretch may directly affect the folding state (see Sohl et al., 1998) of the Na^+ channel protein by lowering a large energy barrier, thereby allowing some domain to assume a previously inaccessible low energy secondary or tertiary conformation. This would be a "ratchet" mechanism: the rate for the backward reaction for the stretch-sensitive transition would be vanishingly small even in the absence of tension. In this, it would differ from stretch-activation or inactivation. The fact that the post-stretch mode coincides with the stable $\alpha + \beta$ mode lends appeal to the idea that stretch provides one-way access to a standard energetically favored folding state of the channel. This is not consistent with a view that the gating modes are at thermal equilibrium.

Second, stretch may change constituents of the bilayer such that the molecular species adjacent to the channel protein (see, e.g., Casado and Ascher, 1998; Shyng and Nichols, 1998), thereby affecting the channel's stability in various states. It would be interesting to test how the partitioning of amphipathic molecules into one leaflet of the bilayer, a bilayer perturbation that has been shown to activate various MS channels (Martinac et al., 1990; Casado and Ascher, 1998; Patel et al., 1998), would affect sodium channel gating modes.

Third, stretch may irreversibly alter some channel cytoskeleton interaction. There is good evidence (Gee et al., 1998) that in its native environment, the Skm Na^+ channel α subunit is linked, via a C terminal PDZ-binding domain, to the dystrophin-actin membrane skeleton and thence to the extracellular matrix. To what extent if at all the oocyte provides endogenous substrates for such linkages is unknown, but it seems plausible that prolonged membrane stretch could disrupt linkages, rendering the channel more susceptible to changes in the bilayer in which it is embedded.

Fourth, membrane stretch may affect some as yet unidentified membrane-delimited second messenger system that modulates the channel. An intriguing candidate for such a second messenger system is the G protein $\beta\gamma$ subunit. Coexpression of G protein $\beta\gamma$ subunits with rat brain type II α subunits in tsA-201 cells elicits large persistent Na^+ currents whose steady-state inactivation is shifted 37 mV in the depolarizing direction (Ma et al., 1997). It would be interesting to test whether endogenous G protein $\beta\gamma$ subunits are responsible for slow gating of Na^+ channels in *Xenopus* oocytes. If so, a tension-induced dissociation of G protein $\beta\gamma$ subunits from Na^+ channel α subunits might be the mechanism whereby stretch converts slow-to-fast gating. Alternately, tension might act by a quite different mechanism, for example, driving prenylated G protein $\beta\gamma$ out of the plasma membrane (this would fall under the second class of mechanism, above). In this case, other membrane-delimited G protein $\beta\gamma$ dependent processes should exhibit irreversible stretch sensitivity. Two channels whose activities are reported as tension-sensitive (albeit not irreversibly) and as G protein $\beta\gamma$ dependent are GIRK (Ji et al., 1998; Nakajima et al., 1996) and voltage-gated Ca^{2+} (Langton, 1993; Clapham, 1996) channels. Finally, we have not ruled out the possibility that, in addition to the slow-to-fast mode conversion, stretch had other irreversible (or poorly reversible) effects such as rundown of a small portion of the channels.

As an aside, we note that since pressure in excess of ~ -10 mmHg applied for seal formation affects the kinetics of various types of ion channels expressed in *Xenopus* oocytes (in particular, Na^+ channels, but also the endogenous MS cation channel (Hamill and McBride, 1997)) one should monitor seal-making procedures as a possible source of patch-to-patch variability in this system.

Is the Na^+ channel α subunit mechanosusceptible?

The swift tension-induced conversion from slow to fast Na^+ channel gating indicates that the α subunit is capable of both gating modes; it rules out the possibility that the modes reflect channel subtypes arising, e.g., from incomplete post-translational modification or premature cessation of protein synthesis. Nonetheless, as indicated in the section above, it is uncertain whether the effects of elevated membrane tension on the sodium channel α subunit reflect direct mechanosusceptibility of the α subunit itself or mechanosensitive processes operating indirectly on the protein. Observations such as ours, but obtained for the α subunit reconstituted into liposomes, would be needed to establish irrefutably that channel protein is susceptible to bilayer tension.

Ruled-out explanations for the stretch effect

Although a mechanically induced gating mode change has not been previously reported for Na^+ channels, a time-dependent shift toward fast gating has been observed in single channel recordings (Zhou et al., 1991): in all long ($>$12 min) patch recordings (both cell-attached and outside-out) channels tended to switch to fast gating by the end of

the recording. Data presented in Moorman et al. (1990, Fig. 4) display a similar pattern. In a preliminary report, Shcherbatko and Brehm (1998) noted a slow (20 min) conversion of the slow gating mode into fast gating mode in macropatches but not in regular patches (like the ones we used); patch excision accelerated the conversion to the fast gating mode. Our findings are not explained by this slow trend, since the mode shift we report was swift in the presence of pressure and was discontinued when pressure was released. However, it is plausible that our findings and the unexplained slow trend of others may be mechanistically related via previously unrecognized effects of voltage on patch tension. Mosbacher et al. (1998) have shown that changes in voltage can lead to movement of the membrane in a patch pipette. An interesting possibility is, therefore, that the prolonged hyperpolarization used to keep the Na^+ channels in a resting state results in increased patch tension. In line with this possibility, Gil et al. (1999) report that prolonged pipette depolarization activates the endogenous MS channels of oocytes in a manner most readily explained if the sustained voltage increases patch tension. Also, it should be noted that various workers dealing with MS channels have found (using MS channel activity as an assay) that patches can have several mmHg of unexplained residual tension and that patch excision or disruption of the cytoskeleton by chemical treatment often results in increased activity of MS channels, probably reflecting increased membrane tension (Sachs and Morris, 1998).

We describe the effects of stretch on cell-attached patches, but the effects were also observed in excised inside-out patches exposed to high K^+ bath solution (not shown). This indicates that involuntary excision of the patch is not an explanation for the effects. It also indicates that the mechanisms involved are 1) localized in the patch and 2) not dependent on characteristics of the membrane cytoskeleton that could be impaired by excision nor on subtle spatial relations of the channel to any cytoplasmic component. In order to know the precise patch voltage, we zeroed the resting membrane potential using high K^+ bath solutions. Prolonged exposure of oocytes to external high K^+ was not instrumental in the stretch effects since the same effects were also obtained (not shown) in cell-attached patches when the bath solution was normal external solution.

A good indication that the speeded-up gating—which we interpret as a slow-to-fast conversion—was not caused by some voltage clamp artifact (e.g., with stretch, channels may become "crowded" and trigger the activation and inactivation of neighboring channels) is the fact that, for the stretch-induced fast mode, not only activation and inactivation, but also recovery from inactivation were all faster. Also, during stretch conversion, the induced fast currents could not have been a clamp artifact produced by an unintended rightward shift in the voltage dependence of slow inactivation since this process was much slower than fast mode inactivation at any voltage, even +50 mV. By the same argument, a voltage clamp artifact would not account for the fast gating associated with high levels of channel expression.

Slow-to-fast ratios in oocytes expressing channels at low versus high levels

The stretch conversion of Na^+ channel gating toward the fast mode suggests scenarios that might explain why low expressing oocytes had exclusively or predominantly slow currents (as seen for spontaneous patches) whereas high expressing oocytes had some slow current but predominantly showed fast ones. One scenario is that vesicle fusion and/or subsequent membrane retrieval (the last steps associated with expression of a membrane protein) transiently and locally elevates membrane tension, promoting the irreversible slow-to-fast conversion of α-subunits already in the membrane: higher levels of expression would augment the number of such local tension transients. Another possibility is saturation of some endogenous molecule, i.e., at high levels of Na^+ channel expression, some endogenous regulatory molecule that generates slow gating when bound to channel protein (e.g., G protein $\beta\gamma$, a membrane skeleton component) is already titrated down.

The β subunit

A salient feature of the stretch effect on Na^+ channel α subunits is that, for the parameters we measured, stretch perfectly mimics the effect of co-expressing the α and β subunits. Thus, the presence of the Na^+ channel's auxiliary subunit and a history of membrane stretch affect gating kinetics and voltage dependence to yield a channel with the same behavior. As was suggested for stretch, it may be that in the presence of the β subunit, α subunit folding, or its interaction with the lipid bilayer or with membrane-bound modulators, is altered.

Both human and rat SkM1 α subunits yield abnormally slow inactivation in oocytes, but normal inactivation in mammalian cell lines (Chahine et al., 1994; Ukamodu et al., 1992); in neither expression system is there evidence for endogenous Na^+ channel β subunits. This discrepancy between oocytes and cell lines is shared by brain but not by cardiac α subunits, which inactivate rapidly in oocytes (Qu et al., 1995). The fact that we could obtain "pure" slow currents in oocytes and then, by applying stretch, convert them to fast currents provides further evidence that the β subunit is not necessary for fast gating.

Possible physiological and pathological significance of stretch effects

Though the magnitude of the patch tension in our experiments was not known, irreversible stretch effects on Na^+ channels occurred over the same range of tensions that reversibly activate the endogenous mechanosensitive (MS) cation channels and that irreversibly abolish the rapid ad-

aptation of that channel. In that experimental sense, the tensions we used were not extreme. However, it is inappropriate to assume that patch stretch is of "physiological" intensity, particularly when it is sustained for minutes, as in our experiments.

Nevertheless, the fact that transient elevated membrane tension can dramatically and, in the case of the Na^+ channel, irreversibly (up to 30 min in our experiments) change the behavior of channels, suggests they may need to avail themselves of various forms of mechanoprotection. Skeletal muscle Na^+ channels bind via G-ankyrin to β-spectrin filaments (Wood and Slater, 1998) and α subunits of Skm1 link to the dystrophin-actin membrane skeleton (Gee et al., 1998). These arrangements localize the channel in appropriate densities at junctional, peri-junctional, and extrajunctional regions. Whether these specific linkages are designed so that the membrane skeleton and extracellular matrix spare the bilayer from mechanical loads is still unknown. Terakawa and Nakayama (1985) have, however, provided evidence that voltage-gated Na^+ and K^+ channels rely on the submembranous cytoskeleton for mechanoprotection. Electronmicroscopy plus current and voltage clamp of internally perfused squid axons showed that after removal of the submembranous skeleton by chaotropic anions (e.g., Cl^-, as KCl), transient inflation (stretch) reversibly abolished the action potential. Voltage-gated currents became impaired only if the naked membrane was mechanically stressed. Axons perfused with KF (not chaotropic) were not stretch-sensitive in this way. These adverse effects of stretch on excitability are unexplained, but the observations suggest that an intact membrane skeleton prevents malfunction of integral membrane proteins by preventing bilayer loading. Most procedures that traumatize the membrane skeleton increase the mechanosusceptibility of TREK-like potassium channels (Wan et al., 1999) and of NMDA channels (Paoletti and Ascher, 1994), again, suggesting that the intact membrane skeleton is a "shock absorber."

Modulation of slow currents may have both physiological and pathological consequences. In various neuronal preparations, a slow, noninactivating, or persistent component of the Na^+ current is thought to be important for integrating signals (Taylor, 1993). Slow Na^+ currents provide the molecular mechanism of inherited cardiac arrhythmia (Bennett et al., 1995) and of hyperkalemic periodic paralysis (Cannon et al., 1995). Identifying the mechanism by which membrane stretch can cause the striking conversion of Na^+ channel gating from slow to fast may lead to the discovery of novel mechanisms of modulation of Na^+ channels or throw light on how the α subunit interacts with other Na^+ channel subunits or with other regulatory molecules.

We thank Dr. Len Maler for reading the manuscript and Cicely Gu for preparing the cRNA.

This work was supported by grants to CEM from the MRC, Canada and from NSERC, Canada.

REFERENCES

Auld, V. J., A. L. Goldin, D. S. Krafte, J. Marshall, J. M. Dunn, W. A. Catterall, H. A. Lester, N. Davidson, and R. J. Dunn. 1988. A rat brain Na^+ channel α subunit with novel gating properties. *Neuron*. 1:449–461.

Bennett, P. B., N. Makita, and A. L. George, Jr. 1993. A molecular basis for gating mode transitions in human skeletal muscle Na^+ channels. *FEBS Lett.* 326:21–24.

Bennett, P. B., K. Yazawa, N. Makita, and A. L. George, Jr. 1995. Molecular mechanism for an inherited cardiac arrhythmia. *Nature*. 376: 683–685.

Cannon, S. C., L. J. Hayward, J. Beech, and R. H. Brown, Jr. 1995. Sodium channel inactivation is impaired in equine hyperkalemic periodic paralysis. *J. Neurophysiol.* 73:1892–1899.

Cannon, S. C., A. I. McClatchey, and J. F. Gusella. 1993. Modification of the Na^+ current conducted by the rat skeletal muscle alpha subunit by coexpression with a human brain beta subunit. *Pflugers Arch.* 423: 155–157.

Casado, M., and P. Ascher. 1998. Opposite modulation of NMDA receptors by lysophospholipids and arachidonic acid: common features with mechanosensitivity. *J. Physiol. (Lond.)*. 513:317–330.

Chahine, M., P. B. Bennett, A. L. George, Jr., and R. Horn. 1994. Functional expression and properties of the human skeletal muscle sodium channel. *Pflugers Arch.* 427:136–142.

Clapham, D. E. 1996. Intracellular signaling: more jobs for G beta gamma. *Curr. Biol.* 6:814–816.

Cota, G., and C. M. Armstrong. 1989. Sodium channel gating in clonal pituitary cells. The inactivation step is not voltage dependent. *J. Gen. Physiol.* 94:213–232.

Favre, I., E. Moczydlowsky, and L. Schild. 1995. Specificity for block by saxitoxin and divalent cations at a residue which determines the sensitivity of sodium channel subtypes to guanidinium toxins. *J. Gen. Physiol.* 106:203–229.

Fleig, A., P. C. Ruben, and M. D. Rayner. 1994. Kinetic mode switch of rat brain IIA Na channels in Xenopus oocytes excised macropatches. *Pflugers Arch.* 427:399–405.

Gee, S. H., R. Madhavan, S. R. Levinson, J. H. Caldwell, R. Sealock, and S. C. Froehner. 1998. Interaction of muscle and brain sodium channels with multiple members of the syntrophin family of dystrophin-associated proteins. *J. Neurosci.* 18:128–137.

Gil, Z., K. L. Magleby, and S. D. Silberberg. 1999. Membrane–pipette interactions underlie delayed voltage activations of mechanosensitive channels in *Xenopus* oocytes. *Biophys. J.* 76:3118–3127.

Gonoi, T., and B. Hille. 1987. Gating of Na channels. Inactivation modifiers discriminate among models. *J. Gen. Physiol.* 89:253–274.

Gu, C. X., P. Juranka, and C. E. Morris. 1998. Mechanical effects on *Shaker*-IR currents. *Biophys. J.* 74:236*a*. (Abstr.).

Hamill, O. P., A. Marty, E. Neher, B. Sakmann, and F. J. Sigworth. 1981. Improved patch-clamp techniques for high-resolution current recording from cells and cell-free membrane patches. *Pflügers Arch.* 391:85–100.

Hamill, O. P., and D. W. McBride, Jr. 1997. Induced membrane hypo/hyper-mechanosensitivity: a limitation of patch-clamp recording. *Annu. Rev. Physiol.* 59:621–631.

Hartshorne, R. P., and W. A. Catterall. 1984. The sodium channel from rat brain: purification and subunit composition. *J. Biol. Chem.* 259: 1667–1675.

Hebert, T. E., R. Monette, R. J. Dunn, and P. Drapeau. 1994. Voltage dependencies of the fast and slow gating modes of RIIA sodium channels. *Proc. R. Soc. Lond. B. Biol. Sci.* 256:253–261.

Isom, L. L., K. S. De Jongh, D. E. Patton, B. F. Reber, J. Offord, H. Charbonneau, K. Walsh, A. L. Goldin, and W. A. Catterall. 1992. Primary structure and functional expression of the beta 1 subunit of the rat brain sodium channel. *Science.* 256:839–842.

Ji, S., S. A. John, Y. Lu, and J. N. Weiss. 1998. Mechanosensitivity of the cardiac muscarinic potassium channel. A novel property conferred by Kir3.4 subunit. *J. Biol. Chem.* 273:1324–1328.

Krafte, D. S., A. L. Goldin, V. J. Auld, R. J. Dunn, N. Davidson, and H. A. Lester. 1990. Inactivation of cloned Na^+ channels expressed in *Xenopus* oocytes. *J. Gen. Physiol.* 96:689–706.

Krafte, D. S., T. P. Snutch, J. P. Leonard, N. Davidson, and H. A. Lester. 1988. Evidence for the involvement of more than 1 RNA species in controlling the inactivation process of rat and rabbit brain Na^+ channels expressed in *Xenopus* oocytes. *J. Neurosci.* 8:2859–2868.

Krieg, P. A., and D. A. Melton. 1984. Functional messenger RNAs are produced by SP6 in vitro transcription of cloned cDNAs. *Nucleic Acids Res.* 12:7057–7070.

Langton, P. D. 1993. Calcium channel currents recorded from isolated myocytes of rat basilar artery are stretch sensitive. *J. Physiol.* 471:1–11.

Ma, J. Y., W. A. Catterall, and T. Scheuer. 1997. Persistent sodium currents through brain sodium channels induced by G protein beta-gamma subunits. *Neuron.* 19:443–452.

Martinac, B., J. Adler, and C. Kung. 1990. Mechanosensitive ion channels of *E. coli* activated by amphipaths. *Nature.* 348:261–263.

McClatchey, A. I., S. C. Cannon, S. A. Slaugenhaupt, and J. F. Gusella. 1993. The cloning and expression of a sodium channel beta 1-subunit cDNA from human brain. *Hum. Mol. Genet.* 2:745–749.

Methfessel, C., V. Witzemann, T. Takahashi, M. Mishina, S. Numa, and B. Sakmann. 1986. Patch clamp measurements on *Xenopus laevis* oocytes: currents through endogenous channels and implanted acetylcholine receptor and sodium channels. *Pflugers Arch.* 407:577–588.

Moorman, J. R., G. E. Kirsch, A. M. J. Van Dongen, R. H. Joho, and A. M. Brown. 1990. Fast and slow gating of sodium channels encoded by a single mRNA. *Neuron.* 4:243–252.

Mosbacher, J., M. Langer, J. K. Horber, and F. Sachs. 1998. Voltage-dependent membrane displacements measured by atomic force microscopy. *J. Gen. Physiol.* 111:65–74.

Nakajima, Y., S. Nakajima, and T. Kozasa. 1996. Activation of G protein-coupled inward rectifier K^+ channels in brain neurons requires association of G protein beta gamma subunits with cell membrane. *FEBS Lett.* 390:217–220.

Paoletti, P., and P. Ascher. 1994. Mechanosensitivity of NMDA receptors in cultured mouse central neurons. *Neuron.* 13:645–655.

Patel, A. J., E. Honore, F. Maingret, F. Lesage, M. Fink, F. Duprat, and M. Lazdunski. 1998. A mammalian two pore domain mechano-gated S-like K^+ channel. *EMBO J.* 17:4283–4290.

Qu, Y., L. L. Isom, R. E. Westenbroek, J. C. Rogers, T. N. Tanada, K. A. McCormick, T. Scheuer, and W. A. Catterall. 1995. Modulation of cardiac Na^+ channel expression in Xenopus oocytes by beta 1 subunits. *J. Biol. Chem.* 270:25696–25701.

Roberts, R. H., and R. L. Barchi. 1987. The voltage sensitive sodium channel from rabbit skeletal muscle. Chemical characterization of subunits. *J. Biol. Chem.* 262:2298–2303.

Sachs, F., and C. E. Morris. 1998. Mechanosensitive ion channels in nonspecialized cells. *Rev. Physiol. Biochem. Pharmacol.* 132:1–77.

Shcherbatko, A., and P. Brehm. 1998. Physiological function of the voltage-dependent sodium channel requires mechanical stabilization. *Biophys. J.* 74:397*a*. (Abstr.).

Shyng, S. L., and C. G. Nichols. 1998. Membrane phospholipid control of nucleotide sensitivity of KATP channels. *Science.* 282:1138–1141.

Smith, R. D., and A. L. Goldin. 1998. Functional analysis of the rat I sodium channel in *Xenopus* oocytes. *J. Neurosci.* 18:811–820.

Sohl, J. L., S. S. Jaswal, and D. A. Agard. 1998. Unfolded conformations of the α-lytic protease are more stable than its native state. *Nature.* 395:817–819.

Taylor, C. P. 1993. Na^+ currents that fail to inactivate. *Trends Neurosci.* 16:455–460.

Terakawa, S., and T. Nakayama. 1985. Are axoplasmic microtubules necessary for membrane excitation. *J. Membr. Biol.* 85:65–77.

Ukamodu, C., J. Zhou, F. J. Sigworth, and W. S. Agnew. 1992. μ1 Na^+ channels expressed transiently in embryonic kidney cells: biochemical and biophysical properties. *Neuron.* 8:663–676.

Wan, X., P. Juranka, and C. E. Morris. 1999. Activation of mechanosensitive currents in traumatized membrane. *Am. J. Physiol.* 276: C318–C327.

Wood, S. J., and C. R. Slater. 1998. β-Spectrin is colocalized with both voltage-gated sodium channels and ankyrinG at the adult rat neuromuscular junction. *J. Cell Biol.* 140:675–684.

Zhou, J., J. F. Potts, J. S. Trimmer, W. S. Agnew, and F. J. Sigworth. 1991. Multiple gating modes and the effect of modulating factors on the μ1 sodium channel. *Neuron.* 7:775–785.